POZNAN UNIVERSITY OF TECHNOLOGY ACADEMIC JOURNALS
No 104 Electrical Engineering 2020

DOI 10.21008/j.1897-0737.2020.104.0008

Łukasz MAJKA*, Marcin SOWA*

EXCITER FRACTIONAL MODEL AND ITS SUSCEPTIBILITY ON PARAMETER CHANGES

The paper concerns the application of fractional calculus in the modeling of a selected part of a power system generating unit, which is the high frequency AC exciter. The model's fractional derivative-based generalization is recalled. The basis of the estimation process for the model consists of two sets of measurement waveforms. In order to solve the fractional and nonlinear problem – a numerical solver is applied. The solver and the estimation procedure have been both implemented in GNU Octave. The model parameter susceptibility is examined. The changes of each model parameter value is studied in a way that the influence on the model output is observed.

KEYWORDS: exciter, measurements, fractional derivative, parameter estimation, numerical solver.

1. INTRODUCTION

Simulation is the most effective, economical way of improving reflection of real phenomena in almost every aspect of engineering. In particular it can be transferred to the power system stability and safety problems. XXI century technologies and IT solutions supported by increasing CPU power encourage the application of such non-invasive methods. When modeling transient states in a power system a particular significance can be attributed to the reflection of the generating unit, because of its role as an active element [1, 2]. Because of the level of its complexity the generating unit is not modeled as a whole, but rather divided into submodels (Fig. 1). This is mainly beneficial because of the following reasons [3]:
– the number of instantaneously estimated model parameters is reduced,
– the number of signals taken into account during the evaluated mathematical expressions is also reduced,
– it increases the reliability of the extracted model because interferences on its output caused by other modeled components are avoided.

Additionally, the above is possible because of the availability of internal signals.

* Silesian University of Technology

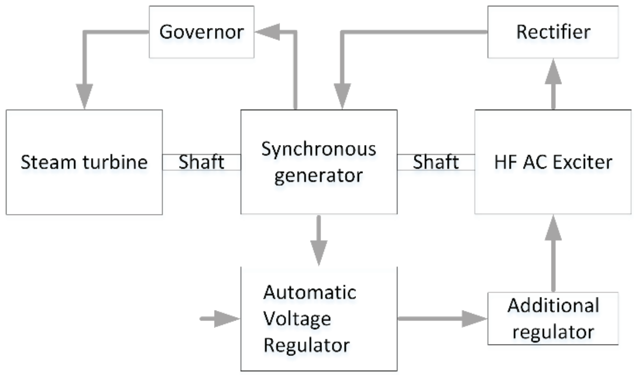

Fig. 1. Generating unit schematic diagram

The submodel of the exciter with an additional regulator provides an appropriate representation of all the features of far more complicated models like that of a synchronous generator, e.g. the influence of gains, time constants, limiters and saturations. In such an analysis the choice of the signals testing the reliability of the model (transients formed in accordance with guidelines given in IEEE standards [4, 5], which the model is required to support) is not coincidental because of their occurrence in tests performed on the real object.

In result of the above one obtains a tool for a reliable determination of the actual set of parameters reflecting the current condition of the component. It is worth to mention that the parameters of the model are constantly changing because of the long-term operation, repairs and modernization of the considered object.

2. EXTENDED EXCITER MODEL APPLYING FRACTIONAL CALCULUS

The studied component can be found within an electromachine excitation system, which is evident in most commonly appearing classes of generating units (associated with the TWW-200 turbogenerator) operating in the Polish Power System. The general idea of the model is constituted by IEEE standards but this particular structure is an original achievement. The process of its invention, testing and modification has been the subject of past papers [2, 3, 6].

The availability of certain well described mathematical foundations and methods, along with computational tools for their evaluation, allow for an improvement of models describing real physical phenomena. One field resulting from such mathematical elements is fractional calculus, which has numerously proven to be useful in modeling when electrical engineering is concerned [7, 8, 9, 10, 11].

When applying fractional derivatives, the previously known model [3] can be extended [6], which results in its more general form as depicted in Fig.2.

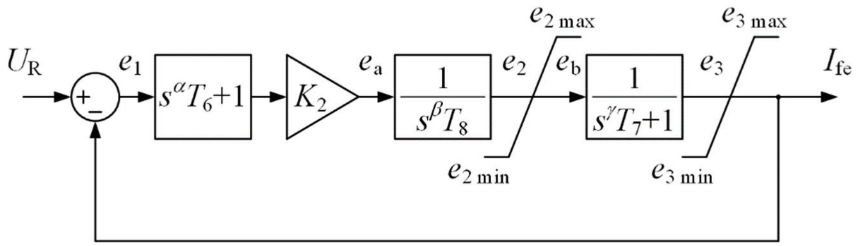

Fig. 2. Fractional order model structural diagram of the exciter with an additional regulator

The introduction of the operators like s^α leads to the fractional derivative, where in this study the Caputo definition (with $\alpha \in [0, 1]$) is considered [12]:

$$ {}_0\mathrm{D}_t^\alpha x(t) = \frac{1}{\Gamma(1-\alpha)} \int_0^t \frac{x^{(1)}(\tau)}{(t-\tau)^\alpha} \mathrm{d}\tau. \tag{1}$$

where the gamma function is applied:

$$\Gamma(z) = \int_0^\infty x^{z-1} \mathrm{e}^{-x}\, \mathrm{d}x. \tag{2}$$

The Caputo definition (next to the Riemann-Liouville definition [13]) is one of the two most commonly applied definitions in analyses of electrical engineering and other engineering fields in general [9, 14, 15, 16].

The differential equations describing the model take the form:

$${}_0\mathrm{D}_t^\alpha e_1(t) = -\frac{1}{T_6} e_1 + \frac{1}{K_2 T_6} e_a, \tag{3}$$

$${}_0\mathrm{D}_t^\beta e_2(t) = \frac{1}{T_8} e_a, \tag{4}$$

$${}_0\mathrm{D}_t^\gamma e_3(t) = \frac{1}{T_7} e_b - \frac{1}{T_7} e_3, \tag{5}$$

with an additional linear equation being:

$$I_{fe} + e_1 = U_R, \tag{6}$$

and the saturation functions (limiting e_2 to $[e_{2\,min}, e_{2\,max}]$ and e_3 to $[e_{3\,min}, e_{3\,max}]$:

$$e_b = \mathrm{sat}_2(e_2), \tag{7}$$

$$I_{fe} = \mathrm{sat}_3(e_3). \tag{8}$$

For the purpose of the analyses in this paper the saturation functions (sat_2 and sat_3) only limit their input variables from the bottom to 0, i.e.:

$$\mathrm{sat}_2(x) = \mathrm{sat}_3(x) = \begin{cases} x & \text{if } x \ge 0, \\ 0 & \text{if } x < 0. \end{cases} \tag{9}$$

3. MEASUREMENT BASIS

The measurement basis is comprised of signals recorded in a power plant generating unit [3]. These constitute actual dynamic waveforms of the basic electric quantities registered during selected test disturbances. One of the commonly applied test disturbances involves a step change of the reference voltage in the automatic voltage regulator (under the synchronous generator no-load condition) by a selected amount. Two tests have been considered, resulting in step changes in alternate directions (an increase and a decrease) for the mentioned quantity. As a result of the introduced test disturbance on the input of the power generator, as far as the exciter is concerned – two measured signals appear: the input signal U_R and the output signal I_{fe}. Initially, the signals contained industrial noise, which has been subjected to filtration [3, 6]. They have also been converted to a per unit system because this is how they are introduced in commercial software dedicated to power system critical analyses [17]. The obtained waveforms (for both test disturbances) have been depicted in Fig. 3.

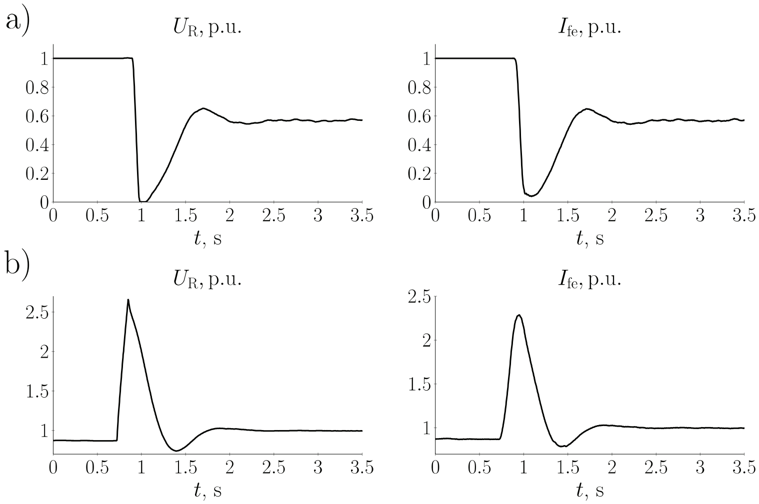

Fig. 3. Input (U_R) and output (I_{fe}) measurement waveforms (in a), b) separately – for different test disturbances)

4. MODEL EVALUATION THROUGH FRACTIONAL PROBLEM SOLUTION

The analysis concerns a transient state and, hence, a single model evaluation requires the solution of the transient nonlinear problem with an input represented by a waveform reconstructed from measurements of $U_R(t)$. The following must be considered in order to determine the proper manner of handling the problem:

- the source time function indicates the need for a tool that can handle arbitrary source waveforms,
- nonlinearities appear in the form of saturation functions: for a general tool being applied currently, and for possible future extensions of these functions to other cases (e.g. arctangent functions), one can consider a tool that can handle nonlinear dependencies between variables,
- fractional derivatives appear; hence, well known ordinary differential equation solvers cannot be applied directly.

There are methods that appear in literature that could handle fractional problems with nonlinearities [18, 19]. However, in most cases specially designed tools would have to be created basing on them as these are not publicly available. The ones that are available are, first off, the adaptive step size solver [20, 21, 22, 23] and its constant step size alternative; secondly – there are also solvers of another author [24, 25, 26]. Because of the authors' familiarity with the first solver – it has been selected for further analysis. It is available in versions for MATLAB and its freeware alternative – GNU Octave. The latter is used in this study.

The solver deals with problems that appear in the general form:

$$\begin{cases} \mathbf{M}_{\mathrm{I}}\mathbf{y}(t)+\mathbf{M}_{\mathrm{II}}\mathbf{x}(t)=\mathbf{T}\mathbf{v}(t)+\begin{bmatrix}\mathbf{0}_{n_y-n_{\mathrm{NL}}}\\ \mathbf{F}_{\mathrm{NL}}(\mathbf{w}(t))\end{bmatrix}, \\ \mathbf{D}^{\boldsymbol{\alpha}}\mathbf{x}(t)+\mathbf{M}_{\mathrm{III}}\mathbf{y}(t)+\mathbf{M}_{\mathrm{IV}}\mathbf{x}(t)=\mathbf{0}_{n_x}, \end{cases} \tag{10}$$

where:

- $\boldsymbol{w}(t)$ is the full solution vector:

$$\mathbf{w}(t)=\begin{bmatrix}\mathbf{y}(t)\\ \mathbf{x}(t)\end{bmatrix} \tag{11}$$

  combining the state vector $\boldsymbol{x}(t)$ (of length n_x) and the vector of the remaining variables $\boldsymbol{y}(t)$ (of length n_y),
- the matrix sizes are as follows: $\boldsymbol{M}_{\mathrm{I}}$ has size $n_y \times n_y$, $\boldsymbol{M}_{\mathrm{II}}$ has size $n_y \times n_x$, $\boldsymbol{M}_{\mathrm{III}}$ has size $n_x \times n_y$, $\boldsymbol{M}_{\mathrm{IV}}$ has size $n_x \times n_x$ and $\mathbf{T}$ has size $n_y \times n_v$,
- $\mathbf{0}_k$ is a notation meaning a column vector of k zeros,
- $\mathbf{D}^{\boldsymbol{\alpha}}\boldsymbol{x}(t)$ is a vector of fractional derivatives of the variables in $\boldsymbol{x}(t)$ (of orders given in $\boldsymbol{\alpha}$),
- $\boldsymbol{F}_{\mathrm{NL}}(\boldsymbol{w}(t))$ is a vector (of length n_{NL}) containing nonlinear dependencies on single variables of $\boldsymbol{w}(t)$; additionally an auxiliary vector $\boldsymbol{i}_{\mathrm{arg}}$ is introduced, which stores the indices of the variables that the subsequent nonlinear functions depend on.

The constant step size alternative of the solver has been applied so that each evaluation concerns the same selected time instances. This is also done to avoid complications, where the selection of a less optimal (in the sense of actual measurement waveform reflection accuracy) set of parameters the solver might pick time instances, where the comparison between the solution and the measurements yields smaller errors and, hence, treating this new set of parameters as more appropriate. The time step size is selected as $\Delta t = 0.02$ s. In further parts of the paper the dependencies on time are only written when there is a need to emphasize them (i.e. as an example: in most cases $U_{\mathrm{R}}(t)$ is written as U_{R}).

For the studied problem $n_y = 3$, $n_x = 3$, $n_v = 1$ and $n_{\mathrm{NL}} = 2$. The solution consists of the two vectors:

$$\mathbf{y} = \begin{bmatrix} I_{\mathrm{fe}} & e_{\mathrm{a}} & e_{\mathrm{b}} \end{bmatrix}^{\mathrm{T}}, \tag{12}$$

$$\mathbf{x} = \begin{bmatrix} e_1 & e_2 & e_3 \end{bmatrix}^{\mathrm{T}}, \tag{13}$$

with the fractional derivative orders:

$$\boldsymbol{\alpha} = \begin{bmatrix} \alpha & \beta & \gamma \end{bmatrix}^{\mathrm{T}}, \tag{14}$$

the source vector consists of one variable:

$$\mathbf{v} = \begin{bmatrix} U_{\mathrm{R}} \end{bmatrix}. \tag{15}$$

The matrices are as follows:

$$\mathbf{M}_{\mathrm{I}} = \begin{bmatrix} 1 & 0 & 0 \\ 0 & 0 & 1 \\ 0 & 0 & 0 \end{bmatrix}, \tag{16}$$

$$\mathbf{M}_{\mathrm{II}} = \begin{bmatrix} 1 & 0 & 0 \\ 0 & 0 & 0 \\ 1 & 0 & 0 \end{bmatrix}, \tag{17}$$

$$\mathbf{M}_{\mathrm{III}} = \begin{bmatrix} 0 & -\dfrac{1}{K_2 T_6} & 0 \\ 0 & 0 & 0 \\ 0 & 0 & -\dfrac{1}{K_2 T_7} \end{bmatrix}, \tag{18}$$

$$\mathbf{M}_{\mathrm{IV}} = \begin{bmatrix} \dfrac{1}{T_6} & 0 & 0 \\ 0 & -\dfrac{1}{T_8} & 0 \\ 0 & 0 & \dfrac{1}{T_7} \end{bmatrix}, \tag{19}$$

$$\mathbf{T} = \begin{bmatrix} 1 & 0 & 0 \end{bmatrix}^{\mathrm{T}}. \tag{20}$$

The vector of nonlinear dependencies:

$$\mathbf{F}_{\mathrm{NL}}(\mathbf{w}) = \left[\mathrm{sat}_2(e_2) \quad \mathrm{sat}_3(e_3)\right]^{\mathrm{T}}, \tag{21}$$

which leads to the auxiliary vector:

$$\mathbf{i}_{\mathrm{arg}} = \left[5 \quad 6\right]^{\mathrm{T}}, \tag{22}$$

because of the dependency on the fifth and sixth variable in $\boldsymbol{w}$ respectively.

5. SUSCEPTIBILITY ON PARAMETER CHANGES

This section concerns a study of the model response on a change in parameter values. This gives some insight on what starting values to choose for the parameters before the actual estimation procedure is executed. The parameter values being studied are given in the vector $\boldsymbol{p}$ with the order being K_2, T_6, T_7, T_8, α, β and γ. Additionally, when one parameter has already been studied (each time 3 values are chosen) then for further parameters the best fit (output of the model versus the measurement waveform) for that parameter remains. The results are depicted in the plots of Fig. 4 up to Fig. 10.

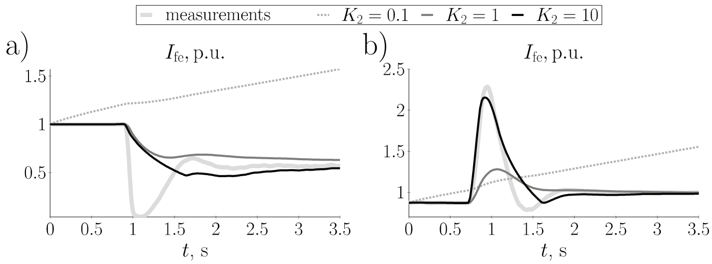

Fig. 4. Study of the susceptibility on changes of K_2 with $\boldsymbol{p}$ = [K_2 1 1 1 0.8 0.8 0.8]

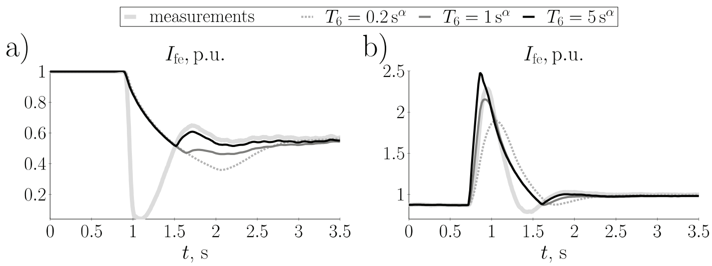

Fig. 5. Study of the susceptibility on changes of T_6 with $\boldsymbol{p}$ = [10 T_6 1 1 0.8 0.8 0.8]

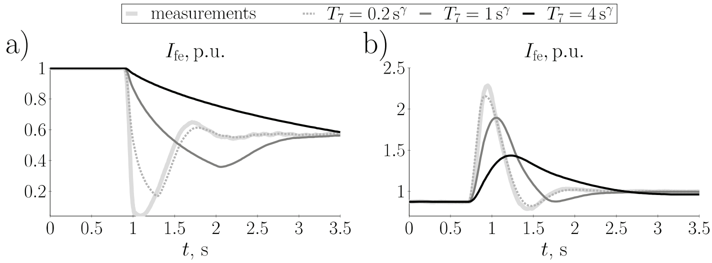

Fig. 6. Study of the susceptibility on changes of T_7 with $\boldsymbol{p}$ = [10 0.2 T_7 1 0.8 0.8 0.8]

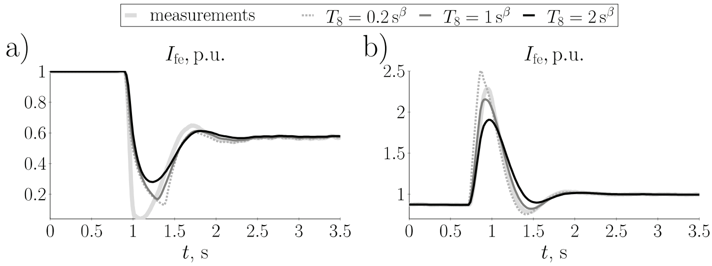

Fig. 7. Study of the susceptibility on changes of T_8 with $\boldsymbol{p}$ = [10 0.2 0.2 T_8 0.8 0.8 0.8]

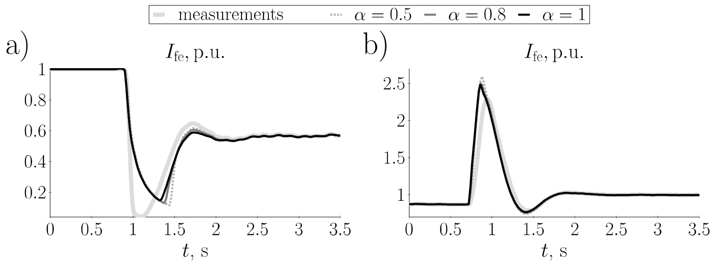

Fig. 8. Study of the susceptibility on changes of α with $\boldsymbol{p}$ = [10 0.2 0.2 0.2 α 0.8 0.8]

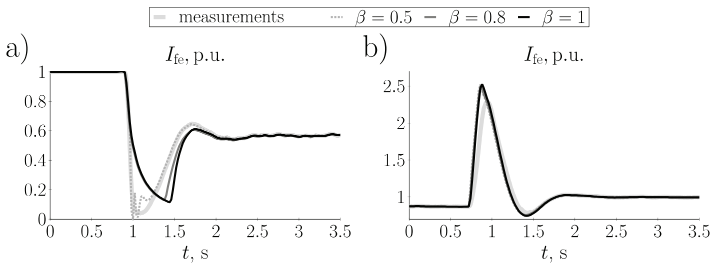

Fig. 9. Study of the susceptibility on changes of β with $\boldsymbol{p}$ = [10 0.2 0.2 0.2 0.8 β 0.8]

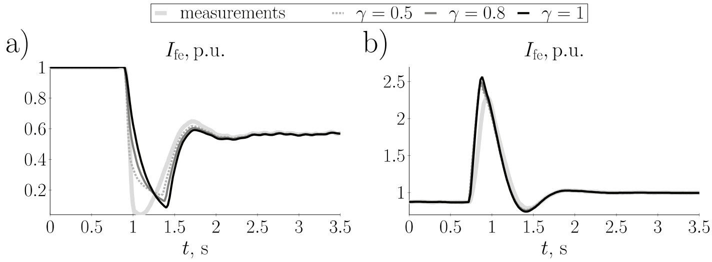

Fig. 10. Study of the susceptibility on changes of γ with $\boldsymbol{p}$ = [10 0.2 0.2 0.2 0.8 0.8 γ]

The starting vector has, hence, the values K_2 = 10, T_6 = 0.2 s$^\alpha$, T_7 = 0.2 s$^\gamma$, T_8 = 0.2 s$^\beta$, α = 0.8, β = 0.8 and γ = 0.8.

6. PARAMETER ESTIMATION AND RESULTS

The parameter estimation procedure has been performed in GNU Octave, where the objective function involved two solutions of the problem described in Section 2 (for different input waveforms of U_R, i.e. for the two different test disturbances described in Section 3), where it has been formulated in terms of the form given by (10) and the numerical solver mentioned in Section 4. The output of the model (i.e. the solution for the variable I_{fe}) is then compared with measurement results. The objective function is a sum of the values computed through the following formula (being computed for the mentioned two solutions):

$$F = \sum_{i=1}^{n} (I_{\mathrm{fe}\,i} - I_{\mathrm{fe\,meas}\,i})^2, \tag{23}$$

where $I_{\mathrm{fe}\,i}$ and $I_{\mathrm{fe\,meas}\,i}$ are the simulation result and the measurement for the selected time instance (with a unique index i). The function being used for the optimization task was *sqp*, which allows for bounded optimization, applying sequential quadratic programming [27]. The Octave script has been, however, more advanced as it involved numerous executions of this function (in a loop) with trials starting from different starting $\boldsymbol{p}$ values: after a successful execution of *sqp*, the next execution is performed with a determined slight random change in the parameters. The lower bounds are given by:

$$p_L = [0.1 \quad 0.01 \quad 0.01 \quad 0.01 \quad 0.2 \quad 0.2 \quad 0.2],$$

while the upper bounds are:

$$p_L = [20 \quad 1 \quad 1 \quad 1 \quad 1 \quad 1 \quad 1].$$

The results of the estimation procedure yielded the following parameters (rounded to 4 significant digits):

$$K_2 = 8.237,\ T_6 = 9.8\cdot 10^{-2}\mathrm{s}^\alpha,\ T_7 = 6.211\cdot 10^{-2}\mathrm{s}^\gamma,\ T_8 = 5.942\cdot 10^{-1}\mathrm{s}^\beta,$$
$$\alpha = 0.8642,\ \beta = 0.9479,\ \gamma = 0.9885.$$

The comparison between the model response for this set of parameters and the measurements of I_{fe} are depicted in Fig. 11 for both studied test disturbances.

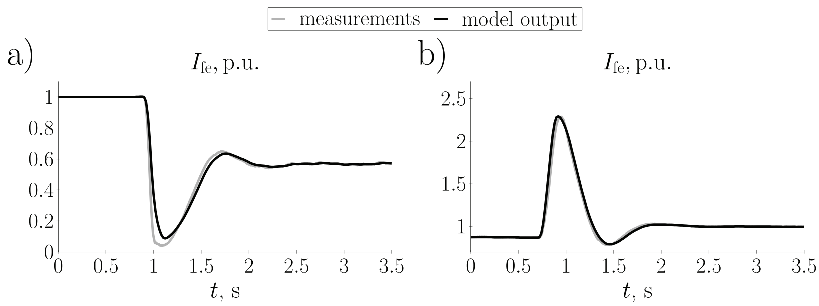

Fig. 11. Comparisons (for both test disturbances) between the measurement waveform and the output waveform of the model

When considering the objective function formula (23) one can define an error (which can be computed for both test disturbances separately):

$$\varepsilon = \sqrt{\frac{F}{n}} \cdot 100\%. \tag{24}$$

The result for the first case is 4.443 %, while for the second the value is 3.967 %. A better reflection of the measurements can also be visually noticed in the case of the second test disturbance.

7. CONCLUSIONS

The study concerned the modeling of high frequency AC exciter with an additional regulator. Its general, fractional derivative-based model has been presented in a structural diagram along with the equations that can be derived from it. The measurement basis has been recalled, which comprised of signals recorded in a power plant generating unit [3]. Two transient conditions of the generating unit have been taken into account as the basis for computations. These two conditions concerned various test disturbances (step changes) of the reference voltage in the automatic voltage regulator, also resulting in specific waveforms for the input signals for the studied object alone (this has been described in Section 3). Each model evaluation, in a later executed estimation procedure, involved the solution of a fractional, nonlinear problem. This has been done through a solver applying the SubIval numerical method [20, 21, 22, 23]. The estimation procedure, executed in GNU Octave, applied the *sqp* function (which allowed for constrained optimization). The result of the analysis shows a good resemblance of the real object response; however, this could be improved. In the previous paper concerning this analysis the model [6] has very accurately reflected one of the transient states (for one test disturbance). In this paper two test disturbances have been applied. This task has proven to be more difficult to match, which is why improvements need to be made in future analyses. One such improvement could be the introduction of nonlinear functions (e.g. arctangent) instead of saturation functions. This improvement will be applied with only some slight modifications as the tool for the numerical computations (described in Section 4) can already handle the solutions of such resulting fractional nonlinear problems.

REFERENCES

[1] Lewandowski M., Majka Ł., Świetlicka A., Effective estimation of angular speed of synchronous generator based on stator voltage measurement.
[2] Paszek S., Boboń A. Berhausen S., Majka Ł., Nocoń A., Pruski P., Synchronous Generators and Excitation Systems Operating in a Power System. Measurement Methods and Modeling. Lecture Notes in Electrical Engineering vol. 631. Cham: Springer, 2020.
[3] Majka Ł., Paszek S., Mathematical model parameter estimation of a generating unit operating in the Polish National Power System. Bull. Pol. Acad. Sci., Tech. Sci. 2016 vol. 64 no. 2, pp. 409–416.
[4] IEEE Guide for Identification, Testing, and Evaluation of the Dynamic Performance of Excitation Control Systems In: IEEE Std 421.2-2014, 2014, pp. 1–63.
[5] IEEE Recommended Practice for Excitation System Models for Power System Stability Studies. In: IEEE Std. 421-5-2016, 2016, pp. 1–207.
[6] Majka Ł., Using fractional calculus in an attempt at modeling a high frequency AC exciter. Advances in non-integer order calculus and its applications. Lecture Notes in Electrical Engineering vol. 559. Cham: Springer, 2020, pp. 55–71.
[7] Majka Ł., Klimas M., Diagnostic approach in assessment of a ferroresonant circuit. Electr. Eng. 2019 vol. 101 iss. 1, pp. 149–164.
[8] Kapoulea S., Tsirimokou G., Psychalinos C., Elwakil A.S., Generalized Fully Adjustable Structure for Emulating Fractional-Order Capacitors and Inductors of Orders less than Two. Circuits, Systems, and Signal Processing, 2019, pp. 1–18.
[9] Majka Ł., Fractional derivative approach in modeling of a nonlinear coil for ferroresonance analyses. Non-integer order calculus and its applications. Lecture Notes in Electrical Engineering vol. 496. Cham : Springer International Publishing, 2019, pp. 135–147.
[10] Dzieliński A., Sarwas G., Sierociuk D., Comparison and validation of integer and fractional order ultracapacitor models. Advances in Difference Equations, 2011:11, 15 pages.
[11] Sowa M., DAQ-based measurements for ferromagnetic coil modeling using fractional derivatives. 2018 International Interdisciplinary PhD Workshop (IIPhDW). Piscataway : Institute of Electrical and Electronics Engineers, 2018, pp. 91–95.
[12] Caputo M., Linear model of dissipation whose Q is almost frequency independent. II. Geophysical Journal International 1967 vol. 13, no. 5, pp. 529–539.
[13] Podlubny I., Fractional Differential Equations. Academic Press, New York, 1999.

[14] Kawala-Janik A., Zolubak M., Bauer W., Nazimek B., Sobolewski T., Martinek R., Sowa M., Pelc M., Implementation of Non-Integer Order Filtration for the Purpose od Disparities Detection in Beta Frequencies – A Pilot Study. 2018 23rd International Conference on Methods & Models in Automation & Robotics (MMAR), 2018, pp. 607–612.
[15] Majka Ł., Applying a fractional coil model for power system ferroresonance analysis. Bull. Pol. Acad. Sci., Tech. Sci. 2018 vol. 66 no. 4, pp. 467-474. Int. J. Electric.l Power. Energ. Syst. 2018 vol. 100, pp. 391–399.
[16] Oprzędkiewicz K., Dziedzic K., Więckowski Ł., Non integer order, discrete, state space model of heat transfer process using Grünwald-Letnikov operator. Bull. Pol. Acad. Sci., Tech. Sci., 2019, vol. 67, no. 5, 905–914.
[17] General Electric, Energy Management System – PSLF – GE Energy Consulting (2018).
[18] Morgado M.L., Ford N.J., Lima P.M., Analysis and numerical methods for fractional differential equations with delay. Journal of Computational and Applied Mathematics, vol. 252, 2013, pp. 159–168.
[19] Li Y., Sun N., Numerical solution of fractional differential equations using the generalized block pulse operational matrix. Computers & Mathematics with Applications vol. 62, 2011, pp. 1046–1054.
[20] Sowa M., Numerical solver for fractional nonlinear circuit problems. IEEE CONCAPAN XXXIX. Convencion de Centro America y Panama, Guatemala, 2019. Piscataway : Institute of Electrical and Electronics Engineers, 2019 (in print).
[21] http://msowascience.com (accessed 31.01.2020)
[22] Sowa M., Dziedzic K., Expansion of a solver for nonlinear fractional problems - the inclusion of time delays. 2019 24th International Conference on Methods and Models in Automation and Robotics (MMAR), 26-29 August 2019, Miedzyzdroje, Poland. Piscataway: Institute of Electrical and Electronics Engineers, 2019, pp. 249–254.
[23] Sowa M., Solutions of circuits with fractional, nonlinear elements by means of a SubIval solver. Non-integer order calculus and its applications. In: Lecture Notes in Electrical Engineering, vol. 496. Cham : Springer. 2019, pp. 217–228.
[24] Garrappa R., Trapezoidal methods for fractional differential equations: Theoretical and computational aspects. Mathematics and Computers in Simulation, vol. 110, 2015, pp. 96–112.
[25] Garrappa R., Numerical Solutions of Fractional Differential Equations: A Survey and a Software Tutorial. Mathematics, vol. 6, no. 2, 2018, 16 pages.
[26] https://www.dm.uniba.it/Members/garrappa/Software
[27] Nocedal J., Wright S.J., Numerical Optimization. Springer Series in Operations Research and Financial Engineering. Springer, Heidelberg, 2006.

(Received: 31.01.2020, revised: 08.03.2020)